

# Poly(ADP-ribosyl)ation of heterogeneous nuclear ribonucleoproteins modulates splicing

Yingbiao Ji and Alexei V. Tulin\*

Fox Chase Cancer Center, Philadelphia, PA 19111, USA

Received December 3, 2008; Revised March 17, 2009; Accepted March 19, 2009

## ABSTRACT

The biological functions of poly(ADP-ribosyl)ation of heterogeneous nuclear ribonucleoproteins (hnRNPs) are not well understood. However, it is known that hnRNPs are involved in the regulation of alternative splicing for many genes, including the *Ddc* gene in *Drosophila*. Therefore, we first confirmed that poly(ADP-ribose) (pADPr) interacts with two *Drosophila* hnRNPs, Squid/hrp40 and Hrb98DE/hrp38, and that this function is regulated by Poly(ADP-ribose) Polymerase 1 (PARP1) and Poly(ADP-ribose) Glycohydrolase (PARG) *in vivo*. These findings then provided a basis for analyzing the role of pADPr binding to these two hnRNPs in terms of alternative splicing regulation. Our results showed that *Parg* null mutation does cause poly(ADP-ribosyl)ation of Squid and hrp38 protein, as well as their dissociation from active chromatin. Our data also indicated that pADPr binding to hnRNPs inhibits the RNA-binding ability of hnRNPs. Following that, we demonstrated that poly(ADP-ribosyl)ation of Squid and hrp38 proteins inhibits splicing of the intron in the *Hsrow-RC* transcript, but enhances splicing of the intron in the *Ddc* pre-mRNA. Taken together, these findings suggest that poly(ADP-ribosyl)ation regulates the interaction between hnRNPs and RNA and thus modulates the splicing pathways.

## INTRODUCTION

Covalent modification of proteins by Poly(ADP-ribose) polymerase (PARP1) has been found to be involved in a variety of biological processes, including DNA repair, apoptosis, and transcription regulation (1). In addition, PARP1-bound poly(ADP-ribose) (pADPr), or free pADPr, is able to bind to proteins through a conserved domain in a non-covalent manner (2). This very stable (3) non-covalent binding to pADPr is equally prevalent in cells and can also modulate protein functions (4–12).

The concentration and size of pADPr within a cell depend on the relative activity of PARP1 and poly(ADP-ribose) glycohydrolase (PARG), which degrades pADPr polymer (13,14). While PARP1 is potentially up-regulated by environmental stress signals, such as DNA damage (1) and heat shock (15), PARP1 is also required for normal development (16,17). PARG plays a key role in recycling automodified PARP1 and maintaining homeostasis of pADPr levels in cells. Thus, PARG loss-of-function in both *Drosophila* and mice causes the accumulation of pADPr which, in turn, results in lethality (13,14,18).

The six major *Drosophila* heterogeneous nuclear ribonucleoproteins (hnRNPs) (*Hrb87F/hrp36*, *Hrb98DE/hrp38*, *Squid/hrp40*, *Hrb27C/hrp48*, *Hrb57A/Bancal* and *hrp59*) have been characterized. Among them, the following hnRNP proteins are similar to the human hnRNP A/B type, which has two RNA-binding domains and one glycine-rich and M9-like (nuclear shuttling signal) domain: *Hrb87F/hrp36* (19); *Hrb98DE/hrp38* (20); *Squid/hrp40* (21) and *Hrb27C/hrp48* (22). *Hrb57A/Bancal* encodes a homolog of the vertebrate hnRNP K protein (23,24), and *Hrp59* encodes a homolog of the vertebrate protein hnRNP M containing three RNA-binding domains (25,26). *Hrp36* (27), *hrp38* (20), *hrp40* (28), *hrp48* (22,29) and *hrp59* (25) have all been shown to be involved in pre-mRNA splicing, and *hrp40* is required for proper RNA localization (21,30,31). Recently, we established that *Hrb98DE/hrp38* is one of the major proteins associated with PARP1 *in vivo* (6). Previously, the human hnRNP A1 protein has been shown to have a pADPr-binding motif and can bind with pADPr by an *in vitro* binding assay (32). However, whether hnRNPs can interact with PARP1 and bind with pADPr *in vivo* is currently unknown. Furthermore, the biological functions of pADPr binding to hnRNPs have not yet been investigated.

Therefore, we use *Drosophila* as the model organism to study the regulation of hnRNPs by poly(ADP-ribosyl)ation. Our data demonstrate that pADPr binding to Squid/hrp40 and Hrb98DE/hrp38 does occur *in vivo* and is, furthermore, regulated by endogenous PARP1 and PARG. In addition, we find that pADPr binding to

\*To whom correspondence should be addressed. Tel: +1 215 728 7408; Fax: +1 215 728 2412; Email: alexei.tulin@fccc.edu

hnRNPs changes the RNA-binding ability of hnRNPs, further modulating splicing.

## MATERIALS AND METHODS

### *Drosophila* strains and breeding conditions

Flies were cultured on standard cornmeal-molasses-agar media at 22°C, unless otherwise indicated. Two *Parp* transgenic lines (*UAST-PARPe-EGFP*; *69B-GAL4/TM3* and *G1-GAL4*, *UAST-PARP1-DsRed*), both having ubiquitous expression of PARP1, were described in our previous reports (15,16). A *Parg* mutant (*Parg27.1/FM7*, *Actin-GFP*) was described previously (13,14). *Hrb98DE/hrp38* GFP trap line (*ZCL588*) and *Squid/hrp40* mutant ( $y^1 w^*$ ;  $P\{lacW\}sqd^{j6E3}$ ,  $l(3)j6E3^{j6E3}/TM3$ ,  $Sb^1$ ) were obtained from the Bloomington *Drosophila* Stock Center. One P-element insertion of the *Hrb98DE/hrp38* gene ( $w^*$ ,  $P\{XP\}d05172/TM6B$ ,  $Tb^1$ ), a *Hrb98DE/hrp38* region deficiency line ( $w^{1118}$ ;  $Df(3R)Exel6209$ ,  $P\{XP-U\}Exel6209/TM6B$ ,  $Tb^1$ ), and a *Parp* mutant (*C03256/TM6B*,  $Tb^1$ ) were obtained from the Exelixis Collection at the Harvard Medical School. We replaced the balancer chromosomes in the *Parp* mutant, the *Squid/hrp40* mutant, the P-element insertion of the *Hrb98DE/hrp38* gene and the *Hrb98DE/hrp38* region deficiency strain with the GFP-bearing balancer from  $w^*$ ;  $Sb1/TM3$ ,  $P\{ActGFP\}JMR2$ ,  $Ser^1$  for selecting the homozygous mutants. We also generated *G1-GAL4*, *UAST-PARP1-DsRed*; *ZCL588* and *Parg27.1/FM7*, *Actin-GFP*; *ZCL588* strains using the standard genetic methods.

### Co-immunoprecipitation

The total proteins from about 25 third-instar wandering larvae of the appropriate genotypes grown at the normal culturing temperature, or heat shocked at 37°C for one hour using water bath, were extracted using RIPA buffer plus protease inhibitor tablets (Roche). The protein concentrations were measured using the RC DC protein assay kit (Bio-Rad). Equal amounts of total proteins (around 1 mg) were precleared with 50 µl protein A agarose (Invitrogen) and 5 µg rabbit IgG (Upstate) for 1 h. The precleared lysate was then precipitated using 5 µg rabbit IgG (the negative control), 5 µg anti-pADPr rabbit polyclonal antibody (Calbiochem) or anti-GFP rabbit polyclonal antibody (Torrey Pines Biolabs) with/without 10 µg RNase A (Sigma) and 100 units RNase T1 (Ambion) per mg protein overnight and further incubated with 30 µl protein A agarose (Invitrogen) for 2 h at 4°C. The IP complex was washed using RIPA buffer five times and eluted with 2× SDS loading buffer at 95°C.

To detect interaction between poly(ADP-ribose) and *hrp38*:GFP fusion protein, a Seize X protein A immunoprecipitation kit (Pierce) was used to eliminate the contamination of the 55 kDa heavy chain of the antibody, which has nearly the same molecular weight as the *hrp38*:GFP fusion protein. Basically, either the rabbit anti-pADPr polyclonal antibody (Calbiochem) or rabbit IgG (Upstate) was covalently crosslinked to immobilized Protein A-beaded agarose resin in a column, according to the protocol provided by the manufacturer (Pierce).

Equal amounts of precleared lysates with 30 µl protein A agarose (Invitrogen) and 5 µg rabbit IgG (Upstate) were precipitated in the column containing the anti-pADPr rabbit polyclonal antibody (Calbiochem) or rabbit IgG (Upstate). The IP complex in the column was washed with RIPA buffer three times and twice with gentle binding buffer (Pierce), then finally eluted with gentle elution buffer (Pierce).

The IP complex obtained, using either the traditional IP method or Seize X protein A immunoprecipitation kit, was subjected to immunoblotting. The blot was incubated with mouse anti-Squid at dilution 1:2500 (8D2; a gift from Dr Dreyfuss) (33), anti-pADPr mouse monoclonal antibody at 1:500 dilution (10H; Calbiochem), anti-DsRed mouse monoclonal antibody at 1:500 dilution (Clontech), and anti-GFP rabbit polyclonal antibody at 1:1000 dilution (Torrey Pines Biolabs) as the primary antibody. After washing the blot with PBS-Tween 20, the blot was further incubated with horseradish peroxidase-conjugated secondary antiserum and detected using ECL<sup>TM</sup> reagents (GE Health). All IPs were repeated twice. The films were photographed with the white light transilluminator (Fisher) using the FoTo/analysis system (FOTODYNE), and the signals were measured using the Image J software (NIH).

### RNA electrophoretic mobility shift assay (EMSA)

RNA EMSA was basically performed according to the protocol provided by the chemiluminescent EMSA kit (Pierce). RNA-binding reaction was done by incubating 100 ng GST (BioVision) or 100 ng GST-hnRNPA1 (Abnova) with 25 fmol biotin-labeled human hnRNP A1 'winner' sequence (UAUGAUAGGGACUUAGGGUG) (34) (Invitrogen) in a 25 µl volume, including 1× binding buffer (10 mM Tris-HCl, 50 mM KCl, 1 mM DTT, pH 7.5), 2.5% glycerol, 2 unit/µl RNAasin (Promega), 0.25 µg/µl purified BSA and 0.25 µg/µl yeast tRNA (Invitrogen) for 30 min at 30°C. For pADPr inhibition assay, 100 ng human GST-hnRNPA1 was preincubated with 70 ng or 140 ng pADPr (Biomol) in 1× binding buffer for 20 min at 25°C. Half of the reaction with 5× loading buffer (Pierce) was run on 6% DNA-retardation gel (Invitrogen) and transferred to the nylon membrane (Hybond-XL, Amersham Biosciences). The free RNA and RNA-protein complex were detected with stabilized streptavidin-horseradish peroxidase conjugate with chemiluminescent substrate (Pierce). EMSA was repeated three times, and the signals were measured using the Image J software (NIH).

### RNA-protein co-immunoprecipitation

The RNA and protein complexes from about 75 third-instar wandering larvae of the appropriate genotypes were extracted using polysome lysis buffer (35). The precleared lysates were incubated with 20 µg anti-GFP rabbit polyclonal antibody (Torrey Pines Biolabs) or 20 µg rabbit IgG (Sigma) (the negative control) overnight at 4°C, followed by precipitating the antigen-antibody complexes with 120 µl protein A agarose (Invitrogen) for 2 h at 4°C. The IP complex was washed three times, using the lysis

buffer, and eluted with 200  $\mu$ l elution buffer [1% SDS, 50 mM NaCl, 50 mM Tris-HCl (pH 7.0), 5 mM EDTA and 100 units/ml RNAase inhibitor (Promega)] at 50°C for 30 min with rocking. RNA from elutes was further precipitated with 800 ml Trizol (Invitrogen) and treated with RQ1 RNAase-free DNase (Promega) and cleaned with RNeasy mini kit (Qiagen) for the regular and real-time RT-PCR assay. The experiment was repeated twice.

### Immunofluorescence

The polytene chromosomes prepared from the salivary glands of the intact nuclei of the wandering third-instar larvae grown at normal culturing temperature, or heat shocked at 37°C for one hour using the water bath, were stained for DNA with DRAQ5 dye (Biostatus). GFP was visualized using the Leica TCS-NT confocal microscope. The method for immunostaining of Squid and pADPr in the polytene chromosome from squashed nuclei was described previously by Tulin and Spradling (15). The primary antibodies were mouse anti-pADPr monoclonal antibody (10H; Calbiochem), used at 1:100 dilution against pADPr, and mouse anti-Squid monoclonal antibody, used at 1:100 dilution (8D2) against Squid. The secondary antibody was Alexa Fluor<sup>®</sup> 488 goat anti-mouse IgG (Invitrogen), used at 1:400 dilution, and propidium iodide (Sigma) was used to stain DNA. The confocal images were quantified using *MetaMorph image analysis* software (Molecular Devices).

### Real-time RT-PCR

Either the wandering third-instar larvae of *yw* (wild-type) or non-GFP homozygous mutants were selected, or allowed to further develop into pharate adults, as indicated, for RNA extraction using RNeasy Mini Kit with on-column DNase digestion (Qiagen). RNA concentration was quantified using the Agilent 2100 BioAnalyzer in combination with an RNA 6000 Nano LabChip (Agilent Technologies). RNA was reverse-transcribed using M-MLV reverse transcriptase (Ambion) and oligo(dT). Real-time PCR assays were performed using Power Sybr<sup>®</sup> Green PCR master mix and an ABI 7900 HT instrument (Applied Biosystems). The primer sequences were as follows: 5' TGAAATAGGAAGCCA GTTGGG3' (forward) and 5' TATCGACTTTTCACGG ATCGAT 3' (reverse) for Hsr $\omega$ -RA; 5' CGAGCTCTTTG TTTGCCTTTC 3' (forward) and 5' CAAAGTCAGGCT GGCGAGA 3' (reverse) for Hsr $\omega$ -RC; 5' CAGTAACT AAAGTGCAACGATCGA 3' (forward) and 5' CCTTTC GCGTATATTCTCCAGATATT 3' (reverse) for Ddc-RB; 5' AACACAATTCCAACAAAACAAACTGA 3' (forward) and 5' GCCTCCATGTTCGATCGAAAC 3' (reverse) for Ddc-RC. As an internal control, the expression level of the *RpL32* gene was measured using the following primers: 5' CCAAGGACTTCATCCGCCACC 3' (forward) and 5' GCGGGTGCCTTGTTCGATCC 3' (reverse). Cycling conditions were 95°C for 15 min, followed by 40 (2-step) cycles (95°C, 15 s; 60°C, 60 s). Ct (cycle threshold) values were converted to quantities (in arbitrary units) using a standard curve (4 points, 5-fold dilutions) established with a calibrator sample. For each

sample per repeat, the value is an average of two PCR reactions performed with inputs of 200 (high input) and 40 ng (lower input) of total RNA. All the experiments were repeated twice, starting from the RNA extractions. The statistics analysis was done based on Student's *t*-test.

## RESULTS

### *Drosophila* hnRNPs have putative pADPr-binding sites

In an effort to identify the target proteins of PARP1, we found that *Drosophila* hrp38 is associated with PARP1 protein using mass spectrometry analysis (6). As previously described (19), hrp38 has 50% identity and conserved functional domains with human hnRNP A1 (Figure 1A). We found that hrp38 contains a pADPr-binding consensus (Figure 1B) previously identified in human hnRNP A1 (32). Squid also has the six residues 'KIFVGG' present in human hnRNP A1, which have been shown to be required for pADPr binding (32). In addition, Squid was also found to have a putative pADPr-binding site (Figure 1B), which is homologous to the pADPr-binding motif identified in human hnRNP M (32). Of added importance to the aims of the present study, we found that both pADPr and Squid accumulated in the ecdysone-inducible E74 and E75 puffs (Figure 1C and D), suggesting the association of pADPr with Squid. Based on these findings, we expected that pADPr could bind to hrp38 and Squid.

### PARP1 overexpression and PARG loss-of-function increases level of pADPr-binding Squid

Using a co-immunoprecipitation strategy (9), we investigated if Squid binds to pADPr *in vivo*. First, we used anti-pADPr antibody to immunoprecipitate the poly(ADP-ribosyl)ated proteins from the wild-type line (*yw*) and immunoblotted the immunoprecipitated complex using the anti-Squid antibody (8D2) (33). The expression level of Squid was strongly reduced in the *Squid* mutant, further confirming the specificity of this Squid antibody (Supplementary Figure S1). The co-immunoprecipitation experiment showed that even the wild-type fly has a modest amount of Squid protein interacting with pADPr (Figure 2A). Since the co-immunoprecipitated Squid protein had the same molecular weight as the native Squid protein (Figure 2A), it appears that pADPr binds with Squid in a non-covalent way. To confirm immunoprecipitation efficiency, we reprobated the same blot with anti-pADPr antibody and observed that there were multiple bands, which are poly(ADP-ribosyl)ated proteins or free pADPr (Figure 2B). We further investigated if pADPr binding to Squid could be impacted by regulating the endogenous PARP1 and PARG. Increases of pADPr-binding Squid protein from two PARP overexpression transgenic lines (*UAS-PARPe-EGFP*; *69B-Gal4* and *G1-Gal4*, *UAS-PARP1-DsRed*) compared to the wild-type, by 2.3 times and 9.4 times, respectively, were observed (Figure 2C). In addition, overexpression of PARP1-DsRed, which represents full PARP activity (16), resulted in a 4-fold increase of pADPr-binding Squid protein over PARPe-EGFP overexpression, which

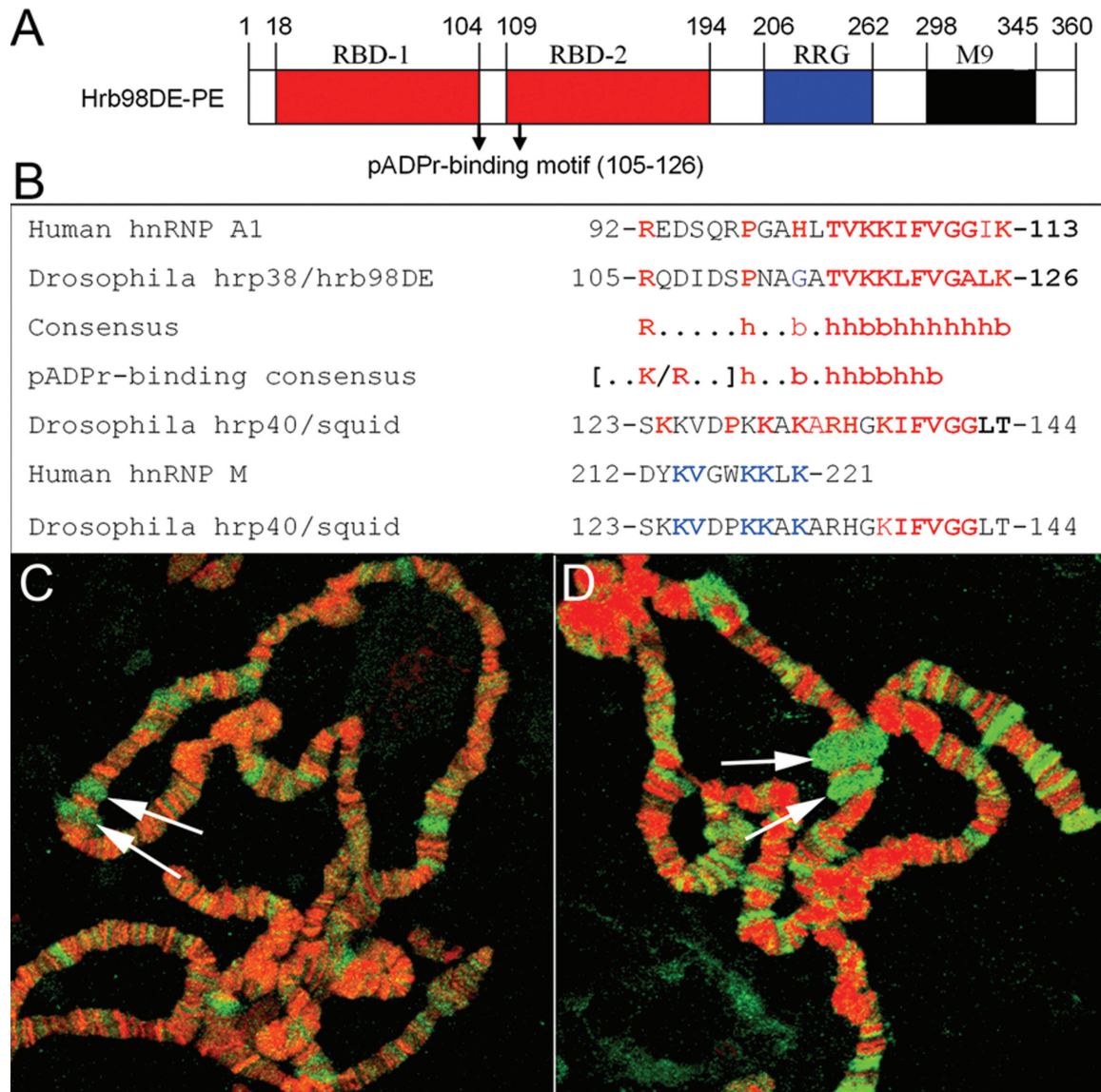


**Figure 1.** The pADPr-binding motif in *Drosophila* Hrp38 and Squid protein. (A) Conserved functional domains of *Drosophila* hrp38 protein. RBD: RNA-binding domains. RRG: glycine-rich domain. M9: nuclear shuttling signal domain. (B) Alignment of putative pADPr-binding sequences of human and *Drosophila* hnRNPs with the consensus of pADPr-binding motif. The conserved residues in the pADPr-binding motif among human hnRNP A1, hrp38 and Squid are marked in red; among human hnRNP M and *Drosophila* Squid, they are marked in blue (b: basic, h: hydrophobic amino acid). (C) The accumulation of pADPr in the puffs. *Drosophila* polytene chromosomes of the wild-type line (*y,w*) were immunostained with the anti-pADPr antibody (10H). pADPr: green; DNA: red. (D) The localization of Squid in the puffs. *Drosophila* polytene chromosomes of the wild-type line (*y,w*) were immunostained with the anti-Squid antibody. Squid: green; DNA: red. Arrows in (C) and (D) indicate the E74 and E75 puffs.

does not have a catalytic domain, but is required for PARP1 transcription (16) and can be modified by PARP1 (6). Indeed, probing the same amount of immunoprecipitated complex from three different genotypes with anti-pADPr antibody showed an increasing order of pADPr level from the PARP overexpression lines (2.0-fold in *UAS-PARPe-EGFP*; *69B-Gal4* and 2.9-fold in *G1-Gal4*; *UAS-PARP1-DsRed*) when compared to the wild-type (*yw*) (Figure 2D). Co-immunoprecipitation experiments also showed that PARG loss-of-function resulted in a 2.7-fold increase of pADPr-binding Squid protein over that of the heterozygous genotype (Figure 2E). Reprobing the same blot with anti-pADPr antibody

showed a greatly increased pADPr level in the *Parg*<sup>-/-</sup> mutant (Figure 2F), indicating that increased Squid bound to pADPr is positively correlated with pADPr accumulation by PARG loss-of-function. Taken together, both PARP overexpression and PARG loss-of-function result in increased amounts of Squid bound to pADPr. Therefore, we conclude that pADPr binding to Squid occurs *in vivo* and is regulated by PARP and PARG.

#### PARP1 overexpression and PARG loss-of-function increase level of pADPr-binding hrp38

Next, to determine if hrp38 binds to pADPr *in vivo*, we generated *G1-GAL4*, *UAS-PARP1-DsRed*; *ZCL588*

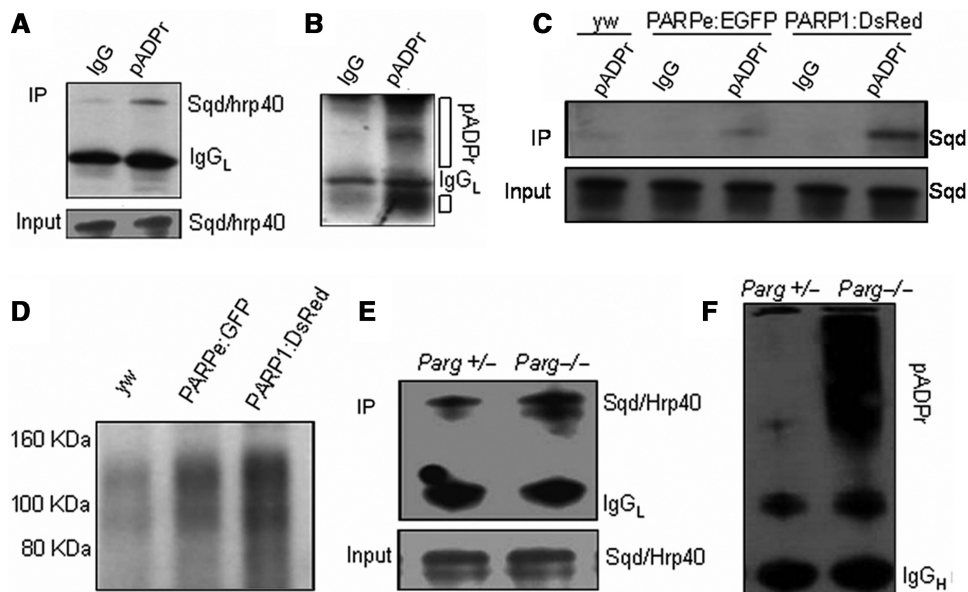


**Figure 2.** Increased amounts of Squid bound to pADPr *in vivo* by PARP overexpression and *Parg* mutation. (A) The total protein from the wild-type line (*yw*) was immunoprecipitated using rabbit anti-pADPr antibody or preimmune rabbit IgG as a negative control. The immunoprecipitates and 1% input for immunoprecipitation were subjected to immunoblotting, using anti-Squid antibody. (B) The same blot was stripped and probed with rabbit anti-pADPr antibody. Open bar indicates pADPr. (C) Equal total proteins from the wild-type line (*yw*), PARPe-EGFP; 69B-Gal4 and G1-Gal4, PARP1-DsRed transgenic lines were immunoprecipitated using rabbit anti-pADPr antibody. The preimmune rabbit IgG was used as a negative control for immunoprecipitation. The immunoprecipitates and 1% input for immunoprecipitation were subjected to immunoblotting analysis using anti-Squid antibody. (D) The same amounts of the immunoprecipitates obtained with rabbit polyclonal anti-pADPr antibody from three different genotypes were immunoblotted with anti-pADPr monoclonal antibody (10H). (E) Equal amounts of the lysates from *Parg*<sup>+/-</sup> heterozygote and *Parg*<sup>-/-</sup> homozygotes were immunoprecipitated using rabbit anti-pADPr antibody. The immunoprecipitates and 1% input for immunoprecipitation were subjected to immunoblot analysis using anti-Squid antibody. (F) The same blot in E was stripped and probed with anti-pADPr monoclonal antibody (10H).

(hrp38:GFP) and *Parg27.1/FM7*, *actin-GFP*; *ZCL588* (hrp38:GFP) strains. *ZCL588* is a protein trap line in which GFP was inserted into the first intron of the *hrp38* (*CG9983*) gene to produce the hrp38:GFP fusion protein (36). Since the *hrp38* (*CG9983*) gene has several alternative transcripts, we sequenced the RT-PCR products from the hrp38:GFP transcripts, and the results showed that GFP was spliced in the frame with hrp38-PE (*CG9983-PE*) (Supplementary Figures S2A and S2B). We used anti-pADPr antibody to immunoprecipitate the poly(ADP-ribosylated) proteins from the *hrp38:GFP* line and *Parp1-DsRed*; *hrp38:GFP* line and further immunoblotted the immunoprecipitated complex using anti-GFP antibody (Figure 3A, Supplementary Figures S2C and S2D). The result showed that pADPr interacts with the hrp38:GFP fusion protein and that there was an average 1.8-fold increase in the level of hrp38:GFP fusion protein bound to pADPr in the PARP1 overexpression transgenic line (*Parp1-DsRed*; *hrp38:GFP*) beyond what was observed in the hrp38:GFP line (Figure 3A). Consistent with the results obtained above, co-immunoprecipitation experiments also showed that *Parg* mutants expressing hrp38:GFP fusion protein (*Parg*<sup>-/-</sup>; *hrp38:GFP*) had a 7.4-fold higher level of fusion protein bound to pADPr than the heterozygous genotype (Figure 3B, upper panel). Probing the same immunoprecipitated complex with the anti-pADPr antibody confirmed immunoprecipitation efficiency

(Figure 3B, bottom panel). Therefore, it appears that pADPr can bind with hrp38, also in a non-covalent way.

#### Automodified PARP1 is associated with hnRNPs *in vivo*

Since PARP1 itself is the predominant acceptor of pADPr, we further determined whether a PARP1-pADPr-Squid complex exists *in vivo*. To make this assessment, we first used anti-GFP antibody to immunoprecipitate the PARPe-EGFP fusion protein from the PARPe-EGFP transgenic line and further immunoblotted the immunoprecipitated complex using anti-Squid antibody. The 40 kDa Squid protein was observed from the immunoprecipitated complex with anti-GFP antibody, but not with preimmune rabbit IgG (Figure 4A), suggesting that an interaction between PARP1 and Squid does take place. The same blot was reprobed with anti-GFP antibody, and the 97 kDa PARPe-EGFP protein was detected, confirming immunoprecipitation efficiency (Figure 4A). Moreover, automodified PARPe-EGFP was also detected in the immunoprecipitated complex using anti-pADPr antibody (Figure 4B), suggesting that the interaction between PARP1 and Squid is mediated by pADPr. In addition, RNase treatment of the lysates did not disrupt the association between Squid and automodified PARPe-EGFP (Figure 4B), confirming that RNA did not mediate the interaction. Secondly, to determine whether an interaction between PARP1 and hrp38 exists *in vivo*, we used anti-GFP antibody to immunoprecipitate the hrp38:GFP

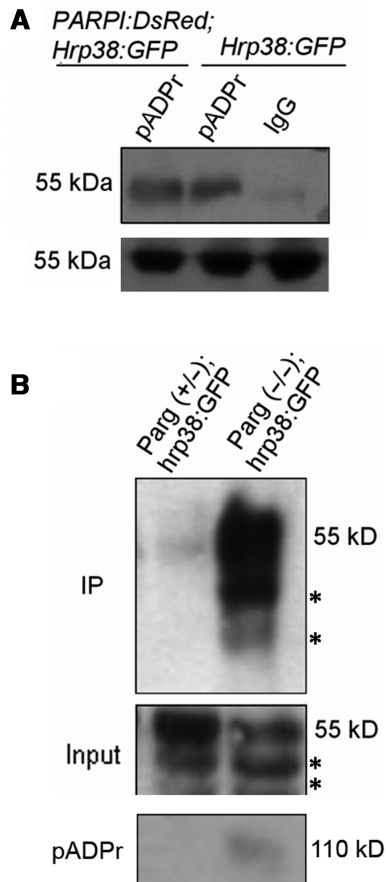


**Figure 3.** Increased amounts of hrp38 bound to pADPr *in vivo* by PARP overexpression and *Parg* mutation. (A) Equal lysates of *hrp38:GFP* and *PARP1-DsRed; hrp38:GFP* transgenic lines were immunoprecipitated using rabbit anti-pADPr antibody or the preimmune IgG crosslinked to protein A agarose beads. The immunoprecipitates and 5% input for immunoprecipitation were subjected to immunoblot analysis using anti-GFP antibody. (B) Equal amounts of the lysates from *Parg*<sup>+/-</sup> heterozygote and *Parg*<sup>-/-</sup> homozygotes were immunoprecipitated using rabbit anti-pADPr antibody crosslinked to protein A agarose beads. The immunoprecipitates (upper panel) and 5% input for immunoprecipitation (middle panel) were subjected to immunoblot analysis using anti-GFP antibody. The same blot in the upper panel was stripped and probed with anti-pADPr monoclonal antibody (bottom panel). Asterisk in upper and middle panel indicates the degraded products from hrp38:GFP.

fusion protein from the PARP1-DsRed; Hrp38:GFP fly strain, followed by immunoblotting the immunoprecipitated complex using anti-DsRed antibody. The PARP1-DsRed fusion protein (~130 kDa) was observed from the immunoprecipitated complex with anti-GFP antibody, but not from the immunoprecipitated complex with preimmune rabbit IgG (Figure 4C). The automodified PARP1-DsRed was also detected in the immunoprecipitated complex using anti-pADPr antibody (Figure 4D). RNase treatment of the lysates did not disrupt the interaction between hrp38 and automodified PARP1-DsRed (Figure 4D), suggesting again that RNA did not mediate this association. Since the expression of hrp38:GFP fusion protein reflects the endogenous expression level of the *hrp38* gene, we concluded that hrp38 is also associated

with automodified PARP1 *in vivo*. Finding an interaction between automodified PARP1 and hrp38 or Squid, in turn, strongly suggests that pADPr binding to Squid or hrp38 is mediated by automodified PARP1 *in vivo*.

### PARP1 controls pADPr binding to Squid during heat shock

Further testing was performed to determine whether PARP1 is required for pADPr binding to hnRNPs, using a partial loss-of-function *PARP1* mutant (C03256), which was verified by northern blot (data not shown). This *PARP1* mutation showed a 3.5-fold lower pADPr level than the wild-type (Figure 5A), further confirming it as a partial loss-of-function *PARP1* mutant. We noticed that there was no obvious difference in the Squid expression level between this *PARP1* mutant and the wild-type (Figure 5A). However, the co-immunoprecipitation experiment showed that this *PARP1* mutant had 2.9-fold less Squid bound to pADPr compared to the wild-type (Figure 5B), further suggesting that PARP1 is required for pADPr binding to Squid. Our previous studies showed that heat shock results in pADPr accumulation at the heat shock-induced puffs (15). Therefore, we tested if heat-shock treatment alters pADPr binding to Squid. As expected, the pADPr level increased by 2.1 times after heat-shock treatment (Figure 5C). Subsequently, even greater amounts of Squid protein bound to pADPr (a 3.9-fold increase) were observed following the heat-shock treatment (Figure 5D), suggesting that the ability of pADPr to bind hnRNPs is up-regulated by the heat-shock treatment. This observation implies that pADPr binding to hnRNPs may play a role in regulating hnRNP upon environmental stresses such as heat shock.

### Poly(ADP-ribosylation) causes the relocation of hnRNPs from chromatin to nucleoplasm

We further examined hrp38 expression patterns in polytene chromosomes prepared from the *Parg; hrp38:GFP* transgenic line. Hrp38 is mainly localized in the puffs and other transcription-activated loci in the hrp38:GFP line (Figure 6A). In the *Parg* mutant nuclei, hrp38:GFP dissociates from the puffs and accumulates in the nucleoplasmic particles (Figure 6B). In wild-type upon heat-shock treatment, hrp38:GFP dissociates from most of the loci and mainly binds to one heat shock-induced puff, *Hsr $\omega$*  (93D) (Figure 6C and Supplementary Figure S3A). It is very likely that hrp38 is sequestered on the 14 kb non-coding RNA (*Hsr $\omega$ -n*) at this locus as other hnRNP proteins (Squid and hrp36) were after heat shock (37). However, in *Parg* mutants, the accumulation of hnRNPs at the *Hsr $\omega$*  (93D) locus is diminished by 3.3 times (Figure 6D). In addition, we found that Squid in the *Parg* mutant also had diminished accumulation by 4.2 times at the *Hsr $\omega$*  (93D) locus upon heat shock (Figure 6F) compared with the wild-type (Figure 6E), suggesting that decreased amounts of Squid bind to the transcript in the *Hsr $\omega$*  (93D) locus. As a control, immunoblotting showed that there is no significant difference in the expression levels of hrp38:GFP and Squid between hrp38:GFP and *Parg; hrp38:GFP* lines after

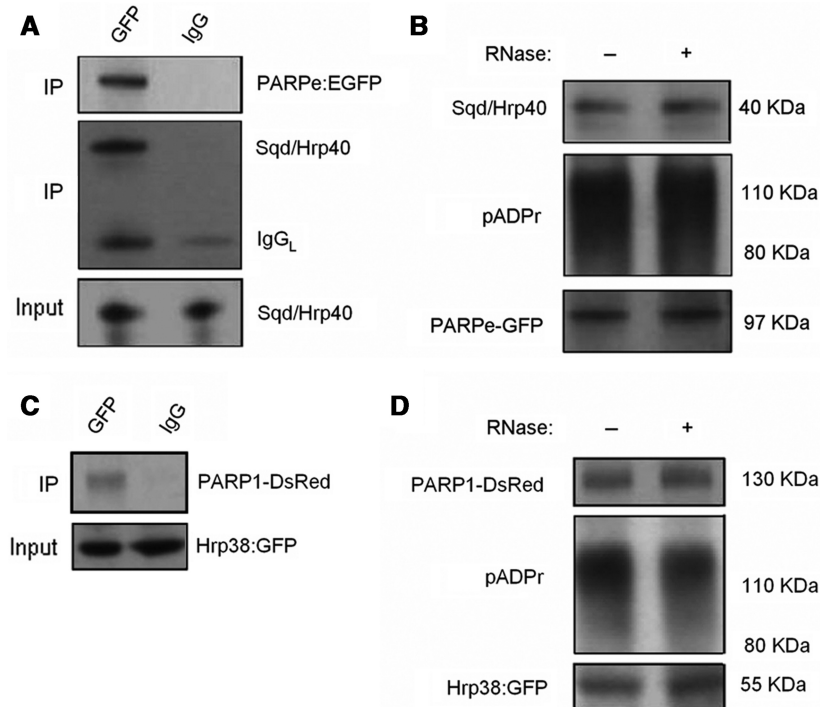


**Figure 4.** The association of PARP with Squid and *hrp38* *in vivo*. (A) An equal amount of lysate from PARPe-EGFP transgenic line was immunoprecipitated using rabbit anti-GFP antibody or preimmune rabbit IgG as a negative control, and the immunoprecipitated complex was subjected to immunoblotting analysis using anti-Squid antibody and reprobbed with mouse anti-GFP antibody. One percent input was shown for the equal amount of protein for immunoprecipitation. (B) Equal amounts of lysates of PARPe-EGFP transgenic line with/without RNase treatment were immunoprecipitated using rabbit anti-GFP antibody. The immunoprecipitated complex was immunoblotted using anti-Squid antibody, anti-pADPr antibody (10H) and anti-GFP monoclonal antibody, respectively. (C) Equal amounts of lysates of the *PARP1-DsRed; Hrp38:GFP* transgenic line were immunoprecipitated using anti-GFP polyclonal antibody, or the normal rabbit IgG, as a negative control, followed by immunoblotting the immunoprecipitated complex using anti-DsRed antibody. Five percent input was immunoblotted using anti-GFP polyclonal antibody to show the equal input. (D) Equal amounts of lysates of the *PARP1-DsRed; Hrp38:GFP* transgenic line with/without RNase treatment were immunoprecipitated using anti-GFP polyclonal antibody. The immunoprecipitated complex was immunoblotted using anti-DsRed antibody and anti-pADPr antibody (10H). Five percent input was immunoblotted using anti-GFP polyclonal antibody to show that *hrp38:GFP* is present in the *PARP1-DsRed; Hrp38:GFP* transgenic line.

heat-shock treatment (Supplementary Figure S3B). Therefore, we proposed that increased pADPr binding to hnRNPs caused by either heat shock or PARG loss-of function alters the RNA-binding ability of hnRNPs because of charge repulsion between pADPr and RNA, which, in turn, results in the dissociation of hnRNPs from most of the transcripts.

#### Poly(ADP-ribose) reduces RNA-binding ability of hnRNPs *in vitro* and *in vivo*

To further test our hypothesis that the interaction between pADPr and hnRNPs reduces the RNA-binding ability of hnRNPs, we used RNA EMSA to determine if pADPr can inhibit human GST-hnRNPA1 binding to its highest-affinity binding ('winner') sequence (34). At first, we confirmed that pADPr can bind with human GST-hnRNPA1 protein using dot-blot analysis (data not shown) as reported before (32). RNA EMSA showed that GST alone did not bind with RNA (Figure 7A, lane 2), while human GST-hnRNPA1 strongly bound with its 'winner' sequence to form the RNA-protein complex (Figure 7A, lane 3) as human hnRNP A1 shown before (38). However, after preincubation of 100 ng GST-hnRNPA1 with 70 ng or 140 ng pADPr (2-fold

excess), the amounts of RNA bound by GST-hnRNPA1 were decreased by 1.8- and 2.7-fold, respectively (Figure 7A, lanes 4 and 5), suggesting that pADPr inhibits human hnRNPA1 binding to RNA in a dosage-dependent manner *in vitro*.

We also tested our hypothesis *in vivo* by co-immunoprecipitating the RNA-hrp38:GFP complex from the wild-type (*hrp38:GFP*) and the *Parg* mutants (*Parg*<sup>27-1</sup>; *hrp38:GFP*) using anti-GFP antibody. The co-immunoprecipitated RNAs were subjected to real-time RT-PCR to amplify a spliced transcript (*Hsrw-RA*) from the *hsrw* (93D) gene. We found that this transcript, *hsrw-RA*, was associated with *hrp38:GFP* and was significantly less co-immunoprecipitated from the *Parg* mutant (*Parg*<sup>27-1</sup>; *hrp38:GFP*) than the wild-type (*hrp38:GFP*) (Figure 7B). Since PARG loss-of function resulted in increased pADPr binding to *hrp38* (Figure 3B), the reduction of the amount of *hrp38:GFP* fusion protein associated with the *hsrw-RA* transcript in the *Parg* mutant suggests that pADPr binding to *hrp38:GFP* abolishes the RNA-binding ability of *hrp38:GFP*. This result also agrees with the observation that *hrp38:GFP* in the *Parg* mutant was relocalized from the puffs at normal temperatures (Figure 6B). Taken together, both RNA EMSA and RNA-protein

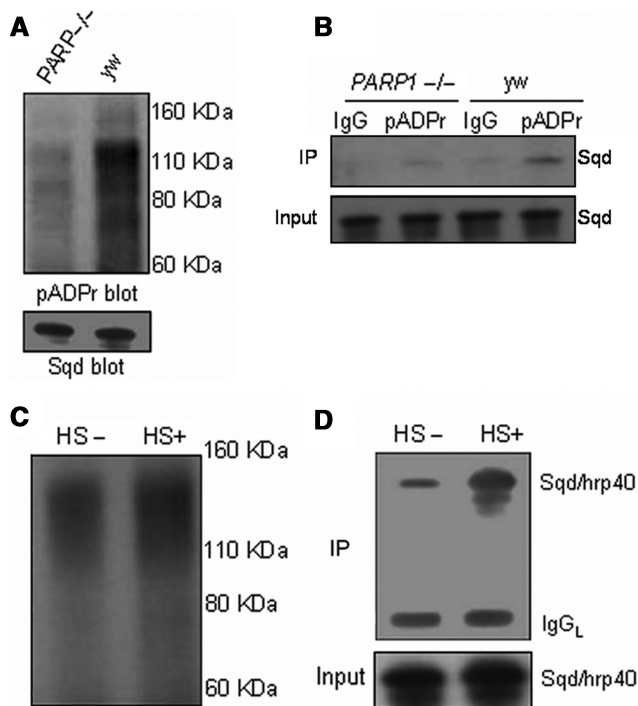


**Figure 5.** pADPr binding to Squid requires PARP1 and is potently induced by the heat-shock treatment: (A) Equal amounts of lysates from the wild-type line (*yw*) and a partial *PARP1* homozygous mutant (*PARP1<sup>-/-</sup>*) were immunoprecipitated with rabbit anti-pADPr antibody. The immunoprecipitates were subjected to immunoblotting with mouse anti-pADPr antibody (10H). One percent input was immunoblotted using anti-Squid antibody to compare Squid expression between wild-type and *PARP1* mutant. (B) Equal amounts of lysates from the wild-type line (*yw*) and a partial *PARP1* homozygous mutant (*PARP1<sup>-/-</sup>*) were immunoprecipitated with rabbit anti-pADPr antibody or rabbit IgG (control). The immunoprecipitates and 1% input were subjected to immunoblotting with anti-Squid antibody. (C) Equal amounts of lysates from the wild-type line (*yw*) grown at 22°C or heat shocked at 37°C for 1 h at the third-instar larvae stage were immunoprecipitated with rabbit anti-pADPr antibody. The immunoprecipitates were subjected to immunoblot analysis using mouse anti-pADPr antibody (10H). (D) The same amount of immunoprecipitates as in Figure C and 1% input for immunoprecipitates were immunoblotted using anti-Squid antibody.

co-immunoprecipitation strongly suggest that pADPr binding to hnRNPs reduces the RNA-binding ability of hnRNPs.

### PARP and PARG modulate splicing *in vivo*

We further predicted that the dissociation of hnRNPs from RNA which results from pADPr binding to hnRNP would, as a consequence, influence pre-mRNA splicing, particularly since the hnRNP family of proteins has been shown to regulate pre-mRNA splicing. To confirm this, we tested the effect of PARG null mutation on the intron splicing in the *hsr $\omega$*  (93D) gene, which encodes a 1.9 kb primary transcript (Hsr $\omega$ -RC) and a 1.2 kb spliced transcript (Hsr $\omega$ -RA) derived from Hsr $\omega$ -RC (39). Using the qRT-PCR assay, the expression level of the Hsr $\omega$ -RC transcript (unspliced) relative to the Hsr $\omega$ -RA transcript (spliced) in the *Parg* mutant and the wild-type (*yw*) was quantified (Figure 8A). The result showed that the ratio

of unspliced transcript (Hsr $\omega$ -RC) to spliced transcript (Hsr $\omega$ -RA) in the *Parg* mutant was 1.5 and 2.6 times greater than that of the wild-type counterpart when compared at the third-instar larvae stage and the pharate stage (Figure 8B, Supplementary Figures S4A and S4B), suggesting that PARG loss-of-function inhibited splicing of Hsr $\omega$ -RC.

We also measured the expression level of the *doublesex* (*dsx-M*) transcript which is derived from alternative splicing of exon 5 in the *dsx* pre-mRNA (40) (Supplementary Figure S5). The results showed that the *Parg* mutant had only 47% and 21% of the *dsx-M* expression level in the control line at the third-instar larvae stage and the pharate stage, respectively, which suggests that PARG loss-of-function likely inhibits splicing exon 5 in the *dsx* pre-mRNA (Supplementary Figures S4A and S5).

In addition, we tested the effect of PARG and PARP on alternative splicing in the *dopa decarboxylase* (*Ddc*) gene. This gene encodes a 2.0 kb completely spliced isoform (Ddc-RC) expressed in the central nervous systems (CNS) and a 1.9 kb alternatively spliced isoform (Ddc-RB) after skipping the second exon, which is mainly expressed in the hypoderm (41) (Figure 8C). Consistent with previous findings (41), we found that the spliced transcript (Ddc-RC) relative to the skipped isoform (Ddc-RB), as expressed in the wild-type, increased about 2-fold after heat shock compared to that under the unstressed condition (Figure 8D). We therefore proposed that heat shock promotes splicing of exon B by displacing splicing repressors from the Ddc-pre-mRNA. To test whether *hrp38* could be a splicing repressor, we characterized a *hrp38* null mutation (*P[XP]d05172*) which has a P-element insertion in the encoding region of the *hrp38* gene and fails to complement a *hrp38* region deficiency (*Df(3R)Exel6209*). We observed that the expression level of the spliced isoform (Ddc-RC) relative to the skipped isoform (Ddc-RB) in both Squid homozygotes (*Sqd<sup>-/-</sup>*) and *hrp38* hemizygote (*Hrp38<sup>-</sup>/Df*) increased around ten-fold compared to the wild-type under the unstressed condition, suggesting that hnRNPs are splicing repressors (Figure 8D and Supplementary Figure S6). Interestingly, both *Parg* mutant and *Parg* overexpression animals (PARPe-EGFP; 69B,GAL4/TM3) also had a very high expression level of the spliced isoform (Ddc-RC) relative to the skipped isoform (Ddc-RB) compared to the wild-type under the unstressed condition (Figure 8D and Supplementary Figure S6), suggesting that accumulation of pADPr enhances splicing of exon B, presumably by increased pADPr binding to the splicing repressors (Hrp38 and Squid). It was also observed that the enhanced splicing effect by heat shock was partially abolished in the *PARP1* mutants (a 50% increase in the *PARP1* mutant versus a two-fold increase in the wild-type) (Figure 8D and Supplementary Figure S6), suggesting that the *PARP1* gene is required for the heat shock-induced splicing regulation. Taken together, we propose that pADPr binding to the splicing repressors (*hrp38* and Squid) on the *Ddc* pre-mRNA results in the dissociation of the splicing repressors from the pre-mRNA, which thereby enhances exon B splicing.

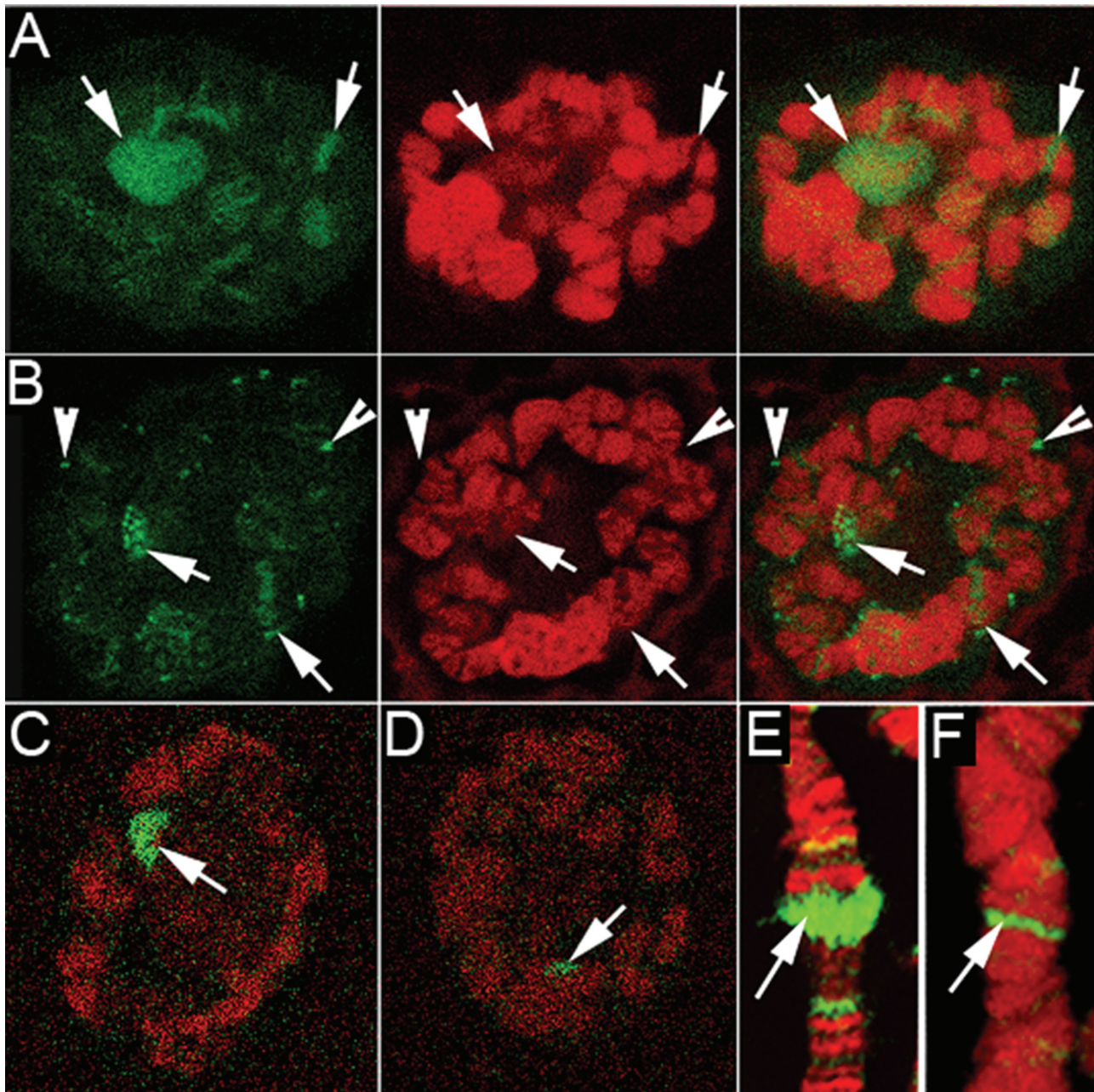


**Figure 6.** The dissociation of hrp38 and Squid from the puffs in polytene chromosomes caused by heat shock and Parg null mutation: hrp38:GFP from the intact nuclei is shown as green in (A) through (D). Squid from the squashed nuclei is shown as green in (E) and (F). DNA is shown as red in (A) through (F). All images are from a single confocal section. (A) The localization of hrp38:GFP in the salivary glands polytene chromosomes of the *hrp38:GFP* transgenic line (ZCL588). Arrows indicate the major puffs. (B) The dissociation of hrp38:GFP from the puffs in polytene chromosomes of *Parg27.1; hrp38:GFP* transgenic lines. Arrowheads indicate extrachromosomal particles accumulating HRP proteins. (C) hrp38:GFP binding to the 93D puff in polytene chromosomes of the *hrp38:GFP* line after heat-shock treatment. Arrow indicates the 93D puff in (C) through (F). (D) Reduced amounts of hrp38:GFP binding to the 93D puff in the *Parg27.1; hrp38:GFP* line after heat-shock treatment. (E) Squid binding to the 93D puff in polytene chromosomes of the wild-type line ( $y^w$ ) after heat-shock treatment: Squid, green; DNA, red. (F) Reduced amounts of Squid binding to the 93D puff in the *Parg27.1* line after heat-shock treatment: Squid, green; DNA, red.

## DISCUSSION

Our results show that pADPr can bind with both Squid and hrp38 in a non-covalent way *in vivo*. We found that PARP1 is required for pADPr binding to Squid, and both PARP1 overexpression and PARG loss-of-function result in increased amounts of hnRNPs bound to pADPr.

We also demonstrated that heat-shock treatment upregulates pADPr-bound Squid as a consequence of the increased pADPr level in the cells. Therefore, our findings demonstrate that the ability of pADPr binding to hnRNPs is subject to regulation by PARP and PARG at the genetic level, as well as physiological conditions *in vivo*, which

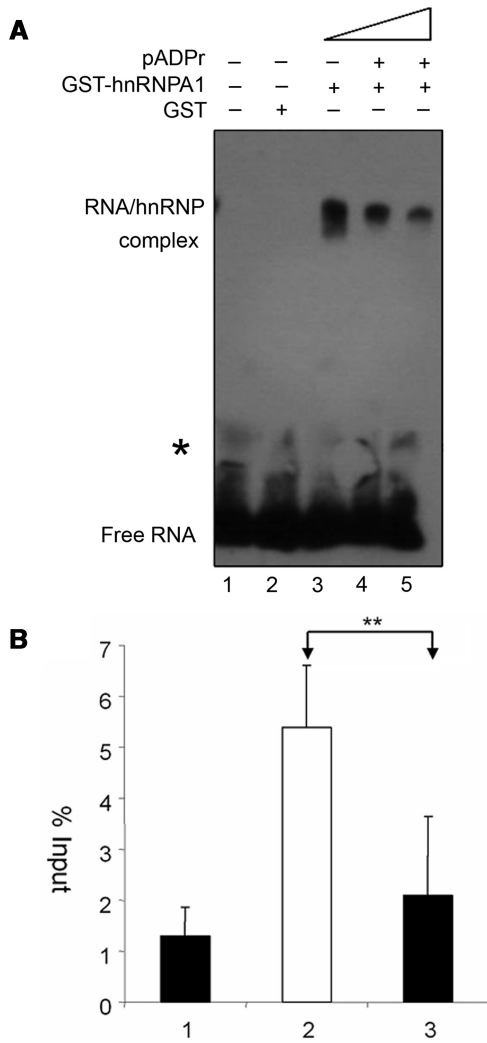


**Figure 7.** Reduced RNA bound to hnRNPs by pADPr and PARG loss-of-function. (A) pADPr inhibits human GST-hnRNPA1 binding to RNA, as shown by EMSA. 25 fmol biotin-labeled hnRNPA1 binding sequence was incubated with the components as indicated: 1. Control; 2. 100 ng GST; 3. 100 ng human GST-hnRNP A1; 4. 100 ng human GST-hnRNP A1 preincubated with 70 ng pADPr; 5. 100 ng human GST-hnRNP A1 preincubated with 140 ng pADPr. \*The trace of higher molecular weight RNA is present in all reactions, which likely comes from the synthetic RNA pool. (B) Reduced RNA bound to hrp38:GFP by PARG loss-of-function. The amount of *hsrw-RA* (spliced product) co-immunoprecipitated with hrp38:GFP as a percent of the input was measured by real-time RT-PCR: 1. *hrp38:GFP* strain immunoprecipitated with IgG as a control; 2. *hrp38:GFP* strain immunoprecipitated with anti-GFP; 3. *Parg27.1; hrp38:GFP* strain immunoprecipitated with anti-GFP. The error bar represents the standard deviation from two independent experiments (\*\* $P \leq 0.01$ ).

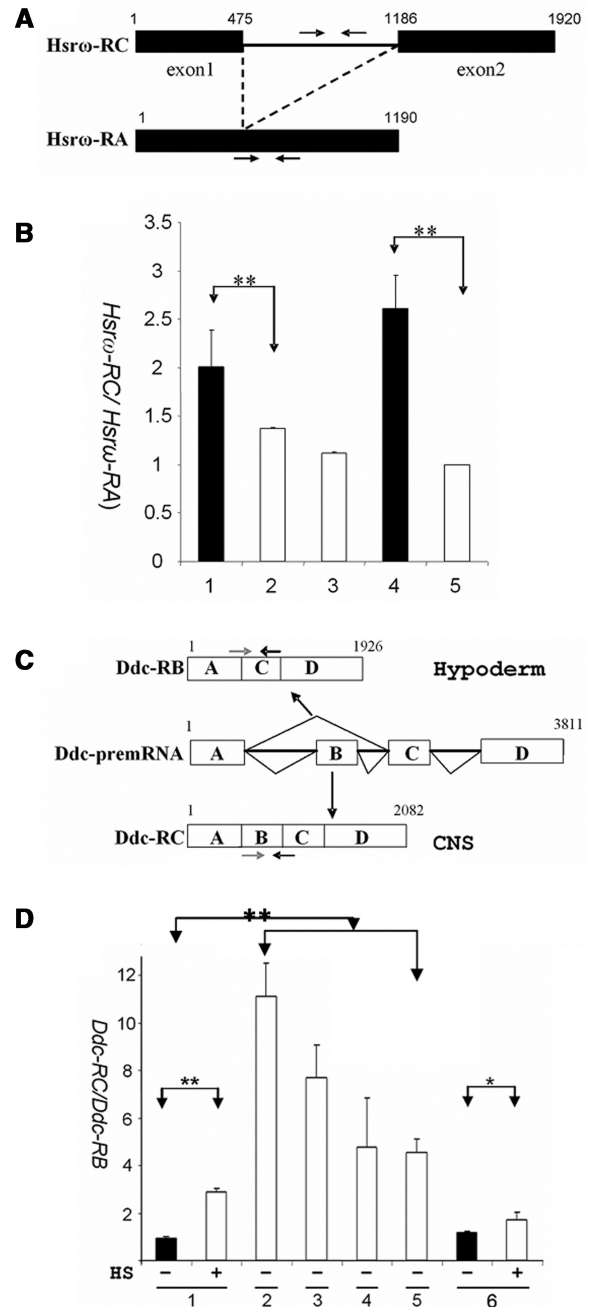


**Figure 8.** Pre-mRNA splicing modulated by PARG and PARG loss-of-function *in vivo*. (A) The structures of Hsrw-RC (unspliced) and Hsrw-RA (spliced) transcripts in the *hsrw* (93D) locus. The primers specific for the intron sequence of Hsrw-RC (black arrow) were used for Hsrw-RC quantification. The forward primer spanning the exon 1 and exon 2 junctions, which are specific for Hsrw-RA, and the reverse primer in the exon 2 of Hsrw-RC and Hsrw-RA were used for Hsrw-RA quantification. (B) The ratios of Hsrw-RC/Hsrw-RA (unspliced to spliced transcript) in the indicated genotypes measured by real-time RT-PCR: 1. *Parg* (-/-), the third-instar larvae male; 2. *yw*, the third-instar larvae male (control); 3. *Parg* (+/-), the third-instar female; 4. *Parg* (-/-), pharate male, and 5. *yw* pharate male (control). (C) The structures of Ddc-RB (skipped isoform) and Ddc-RC (spliced isoform) transcripts in the *Ddc* gene. The positions of isoform-specific primers are indicated with arrows. CNS: central nervous system. (D) The ratios of Ddc-RC/Ddc-RB (spliced to skipped isoforms) in the indicated genotypes and

**Figure 8. Continued**  
treatment measured by real-time RT-PCR: 1. *yw* (the wild-type) as the control; 2. *Squid*<sup>-/-</sup> (*sqd*<sup>*sqd*<sup>6E3</sup></sup>/*sqd*<sup>*sqd*<sup>6E3</sup></sup>); 3. *hrp38*<sup>-/-</sup> (*P[XP]d05172/Df(3R)Exel6209*); 4. *Parg*<sup>-/-</sup> (*Parg* 27.1/*Parg* 27.1); 5. *Parpe-EGFP* (*PARPe-EGFP; 69B-Gal4*); 6. *Parg*<sup>-/-</sup> (*C03256/C03256*). All RNAs were extracted from the third-instar larvae. HS: 1-h heat shock of the third-instar larvae. The error bar represents the standard deviation from two independent experiments. \* $P \leq 0.05$ ; \*\* $P \leq 0.01$ .

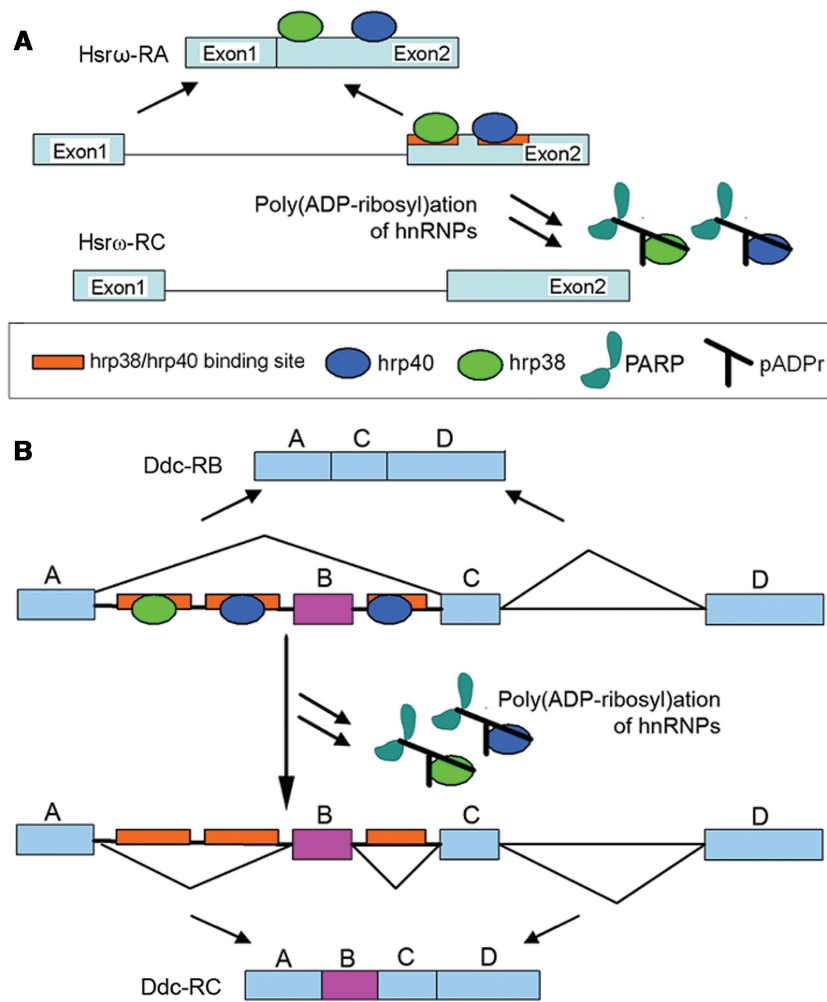


**Figure 9.** The model for the modulation of splicing by hnRNP poly(ADP-ribosylation). **(A)** Splicing inhibition by poly(ADP-ribosylation) of hnRNPs. Hrp38 and Squid bind to the G triplets or quartets as exonic splicing enhancers (ESEs) in exon 2 of the *Hsr $\omega$ -RC* transcript to promote splicing the intron (Supplementary Figure S7). However, the dissociation of hnRNPs from the transcript, such as *Hsr $\omega$  pre-RC*, after poly(ADP-ribosylation) of hnRNPs, inhibits intron splicing. **(B)** Splicing enhancement by poly(ADP-ribosylation) of hnRNPs. In hypoderm tissues, the binding of Hrp38 and Squid to the G triplets or quartets as intronic splicing silencers (ISSs) in introns 1 and 2 of the *Ddc* pre-mRNA inhibits splicing and results in exon skipping. The dissociation of hnRNPs from the transcript, such as the *Ddc* pre-mRNA, by poly(ADP-ribosylation) of hnRNPs induced by heat shock or elevated PARP1 activity in CNS (13), enhances intron splicing.

ultimately determine pADPr synthesis and degradation rates in an organism. This is consistent with the observation that the binding affinity of pADPr to specific proteins depends on the pADPr chain length and branching complexity by *in vitro* studies (3,42).

Heat shock has a dramatic effect on the redistribution of hnRNPs in polytene chromosomes, including Squid (37) and Hrp38 (this report). Upon heat shock, hnRNPs dissociate from most of the transcripts and exclusively bind to one heat shock-induced transcript (*hsr $\omega$ -n*) at the *Hsr $\omega$*  locus, likely serving as the storage speckles (37). Here we propose a model which includes the following steps: (i) pADPr-PARP accumulated after heat shock binds with hnRNPs associated with the transcripts. (ii) This binding, in turn, results in the dissociation of hnRNPs from most of the transcripts as a result of either charge repulsion between pADPr and RNA or abolishment of RNA-binding ability of

pADPr-bound hnRNPs. (iii) Then, a PARP-pADPr-hnRNPs complex moves into the nucleoplasm where PARG cleaves most of the pADPr. (iv) Finally, the free hnRNPs released from the PARP-pADPr complex bind with the non-coding RNA (*hsr $\omega$ -n*) at the *Hsr $\omega$*  locus. Consistent with our model, we observed that diminished amounts of Squid and hrp40:GFP in the *Parg* mutant are sequestered at the *Hsr $\omega$*  (93D) locus upon heat shock. Thus, in the *Parg* mutant, it appears that PARG failed to cleave pADPr after heat shock so that only a minimum of free hnRNPs are available to bind to 93D.

It has been observed that hnRNPs can either promote or inhibit splicing by binding with exonic and intronic splicing enhancers (ESEs and ISEs) and silencers (ESSs and ISSs) (25,43,44). Since pADPr binding to hnRNPs causes the dissociation of hnRNPs from RNA, we have further proposed that splicing is either promoted or inhibited, depending on whether hnRNP binding takes

place with splicing enhancers (ESEs and ISEs) or silencers (ESSs and ISSs) (Figure 9). In agreement with this hypothesis, we first observed that *Parg* null mutation partly inhibited splicing Hsr $\omega$ -RC (Figure 8B) and splicing of the *doublesex* gene (Supplementary Figure S4). Our results also demonstrate that PARG loss-of-function and PARP overexpression can enhance splicing of the *Ddc* pre-mRNA, which is similar to the effect of heat shock on splicing of the *Ddc* pre-mRNA. It is well known that heat shock can inhibit splicing (45,46). However, the effect of heat shock on splicing of the *Ddc* pre-mRNA illustrates that heat shock can also promote splicing (41). Our data strongly suggest that hrp38 and Squid are the splicing repressors for *Ddc* splicing since either hrp38 or Squid null mutation results in a very low expression of the skipped isoform which is produced by splicing inhibition. There are several G triplets or quartets in the intron 1 and intron 2 of the *Ddc* gene, which could be intronic splicing silencers (ISSs) for hrp38 and Squid binding (Supplementary Figure S8). We have observed that heat shock treatment results in increased amounts of hnRNPs bound to pADPr and the dissociation of hnRNPs from most of the transcripts. Based on this evidence, we proposed that heat shock induces the dissociation of the repressors (hrp38 or Squid) from the intronic splicing silencers in the *Ddc* pre-mRNA as a result of pADPr binding to hnRNPs and that this, in turn, enhances splicing of the *Ddc* pre-mRNA (Figure 9B). It has been reported that heat shock can induce dephosphorylation of a serine-arginine-rich splicing factor (SRp38) to inhibit splicing in human HeLa cells (47). Recently, it was also shown that pADPr can bind with human SR splicing factor (ASF/SF2) and further inhibit its phosphorylation (48). Therefore, pADPr binding to hnRNPs induced by heat shock could be an alternative to, or a mechanism combined with, the action of SRp38 dephosphorylation to regulate splicing upon heat shock.

In this report, we did not observe that *Parp* mutation has any effect on splicing at normal physiological condition in the two splicing events analyzed, Hsr $\omega$  and *Ddc* genes. However, it has been reported that mammalian *Parp-1* knockout cells have an increased incidence of alternative splicing within a subset of inflammatory response genes (48). Therefore, we suggest that the proposed model can be extended to explain tissue- or developmental-specific splicing under normal physiological conditions as a consequence of the spatial- and temporal-specific activity of PARP and PARG in the cell. For example, the maximal accumulation of pADPr was observed at the prepupal stage in the wild-type fly (49), and we also observed that both pADPr and Sqd accumulated at E74 and E75 loci (Figure 1C and D) where both genes have several alternative spliced isoforms. Therefore, it is reasonable to infer a dynamic scenario in which pADPr produced by activated PARP1 could transiently bind to hnRNP in puffs for the regulation of splicing at these sites. Further elucidation to confirm the developmental roles of hnRNP poly(ADP-ribosylation) on splicing will be undertaken in future investigation.

## SUPPLEMENTARY DATA

Supplementary Data are available at NAR Online.

## ACKNOWLEDGEMENTS

We thank Dr Dreyfuss for providing materials. Drs K. Zaret, R. Meyer and Mr D. Martin contributed valuable comments on the manuscript.

## FUNDING

National Institutes of Health (R01 GM077452) and the Ellison Medical Foundation (GM27875) [to A.V.T.]. Funding for open access charge: National Institutes of Health (R01 GM077452)

*Conflict of interest statement.* None declared

## REFERENCES

- D'Amours,D., Desnoyers,S., Silva,D. and Poirier,G.G. (1999) Poly(ADP-ribosylation) reactions in the regulation of nuclear functions. *Biochem. J.*, **342**, 249–268.
- Pleschke,J.M., Kleczkowska,H.E., Strohmann,M. and Althaus,F.R. (2000) Poly(ADP-ribose) binds to specific domains in DNA damage checkpoint proteins. *J. Biol. Chem.*, **275**, 40974–40980.
- Panzeter,P.L., Realini,C.A. and Althaus,F.R. (1992) Noncovalent interactions of poly(adenosine diphosphate ribose) with histones. *Biochemistry*, **31**, 1379–1385.
- Poirier,G.G., de Murcia,G., Jongstra-Bilen,J., Niedergang,C. and Mandel,P. (1982) Poly(ADP-ribosylation) of polynucleosomes causes relaxation of chromatin structure. *Proc. Natl Acad. Sci. USA*, **79**, 3423–3427.
- Boulikas,T. (1990) Poly(ADP-ribosylated) histones in chromatin replication. *J. Biol. Chem.*, **265**, 14638–14647.
- Pinnola,A., Naumova,N., Shah,M. and Tulin,A.V. (2007) Nucleosomal core histones mediate dynamic regulation of PARP1 protein binding to chromatin and induction of PARP1 enzymatic activity. *J. Biol. Chem.*, **282**, 32511–32519.
- Mendoza-Alvarez,H. and Alvarez-Gonzalez,R. (2001) Regulation of p53 sequence-specific DNA-binding by covalent poly(ADP-ribosylation). *J. Biol. Chem.*, **276**, 36425–36430.
- Malanga,M., Pleschke,J.M., Kleczkowska,H.E. and Althaus,F.R. (1998) Poly(ADP-ribose) binds to specific domains of p53 and alters its DNA binding functions. *J. Biol. Chem.*, **273**, 11839–11843.
- Saxena,A., Saffery,R., Wong,L.H., Kalitsis,P. and Choo,K.H. (2002) Centromere proteins Cenpa, Cenpb, and Bub3 interact with poly(ADP-ribose) polymerase-1 protein and are poly(ADP-ribosylated). *J. Biol. Chem.*, **277**, 26921–26926.
- Malanga,M. and Althaus,F.R. (2004) Poly(ADP-ribose) reactivates stalled DNA topoisomerase I and induces DNA strand break resealing. *J. Biol. Chem.*, **279**, 5244–5248.
- Reale,A., Matteis,G.D., Galleazzi,G., Zampieri,M. and Caiafa,P. (2005) Modulation of DNMT1 activity by ADP-ribose polymers. *Oncogene*, **24**, 13–19.
- Haince,J.F., Kozlov,S., Dawson,V.L., Dawson,T.M., Hendzel,M.J., Lavin,M.F. and Poirier,G.G. (2007) Ataxia telangiectasia mutated (ATM) signaling network is modulated by a novel poly(ADP-ribose)-dependent pathway in the early response to DNA-damaging agents. *J. Biol. Chem.*, **282**, 16441–16453.
- Hanai,S., Kanai,M., Ohashi,S., Okamoto,K., Yamada,M., Takahashi,H. and Miwa,M. (2004) Loss of poly(ADP-ribose) glycohydrolase causes progressive neurodegeneration in *Drosophila melanogaster*. *Proc. Natl Acad. Sci. USA*, **101**, 82–86.
- Tulin,A., Naumova,N.M., Menon,A.K. and Spradling,A.C. (2006) *Drosophila* poly(ADP-Ribose) glycohydrolase mediates chromatin structure and SIR2-dependent silencing. *Genetics*, **172**, 363–371.

15. Tulin, A. and Spradling, A.C. (2003) Chromatin loosening by poly(ADP)-ribose polymerase (PARP) at *Drosophila* puff loci. *Science*, **299**, 560–562.
16. Tulin, A., Stewart, D. and Spradling, A.C. (2002) The *Drosophila* heterochromatic gene encoding poly(ADP-ribose) polymerase (PARP) is required to modulate chromatin structure during development. *Genes Dev.*, **16**, 2108–2119.
17. Ménéssier-de Murcia, J., Ricoul, M., Tartier, L., Niedergang, C., Huber, A., Dantzer, F., Schreiber, V., Amé, J.C., Dierich, A., LeMeur, M., Sabatier, L., Chambon, P. and de Murcia, G. (2003) Functional interaction between PARP-1 and PARP-2 in chromosome stability and embryonic development in mouse. *EMBO J.*, **22**, 2255–2263.
18. Koh, D.W., Lawler, A.M., Poitras, M.F., Sasaki, M., Wattler, S., Nehls, M.C., Stöger, T., Poirier, G.G., Dawson, V.L. and Dawson, T.M. (2004) Failure to degrade poly(ADP-ribose) causes increased sensitivity to cytotoxicity and early embryonic lethality. *Proc. Natl Acad. Sci. USA*, **101**, 17699–17704.
19. Haynes, S.R., Raychaudhuri, G., Johnson, D., Amero, S. and Beyer, A.L. (1990) The *Drosophila* Hrb loci: A family of hnRNA binding proteins. *Mol. Biol. Rep.*, **14**, 93–94.
20. Shen, J., Zu, K., Cass, C.L., Beyer, A.L. and Hirsh, J. (1995) Exon skipping by overexpression of a *Drosophila* heterogeneous nuclear ribonucleoprotein *in vivo*. *Proc. Natl Acad. Sci. USA*, **92**, 1822–1825.
21. Norvell, A., Kelley, R.L., Wehr, K. and Schupbach, T. (1999) Specific isoforms of Squid, a *Drosophila* hnRNP, perform distinct roles in Gurken localization during oogenesis. *Genes Dev.*, **13**, 864–876.
22. Hammond, L., Rudner, D.Z., Kanaar, R. and Rio, R.C. (1997) Mutations in the hrp48 gene, which encodes a *Drosophila* heterogeneous nuclear ribonucleoprotein particle protein, cause lethality and developmental defects and affect P-element third-intron splicing *in vivo*. *Mol. Cell Biol.*, **17**, 7260–7267.
23. Charroux, B., Angelats, C., Fasano, L., Kerridge, S. and Vola, C. (1999) The levels of the bancal product, a *Drosophila* homologue of vertebrate hnRNP K Protein, affect cell proliferation and apoptosis in imaginal disc cells. *Mol. Cell Biol.*, **19**, 7846–7856.
24. Hovemann, B.T., Reim, I., Werner, S., Katz, S. and Saumweber, H. (2000) The protein Hrb57A of *Drosophila melanogaster* closely related to hnRNP K from vertebrates is present at sites active in transcription and coprecipitates with four RNA-binding proteins. *Gene*, **245**, 127–137.
25. Kiesler, E., Hase, M.E., Brodin, D. and Visa, N. (2005) Hrp59, an hnRNP M protein in *Chironomus* and *Drosophila*, binds to exonic splicing enhancers and is required for expression of a subset of mRNAs. *J. Cell Biol.*, **168**, 1013–1025.
26. Hase, M.E., Yalamanchili, P. and Visa, N. (2006) The *Drosophila* heterogeneous nuclear ribonucleoprotein M protein, HRP59, regulates alternative splicing and controls the production of its own mRNA. *J. Biol. Chem.*, **281**, 39135–39141.
27. Zu, K., Sikes, M.L., Haynes, S.R. and Beyer, A.L. (1996) Altered levels of the *Drosophila* HRB87F/hrp36 hnRNP protein have limited effects on alternative splicing *in vivo*. *Mol. Biol. Cell*, **7**, 1059–1073.
28. Park, J.W., Parisky, K., Celotto, A.M., Reenan, R.A. and Graveley, B.R. (2004) Identification of alternative splicing regulators by RNA interference in *Drosophila*. *Proc. Natl Acad. Sci. USA*, **101**, 15974–15979.
29. Siebel, C.W., Kanaar, R. and Rio, D.C. (1994) Regulation of tissue-specific P-element pre-mRNA splicing requires the RNA-binding protein PSI. *Genes Dev.*, **8**, 1713–1725.
30. Goodrich, J.S., Clouse, K.N. and Schupbach, T. (2004) Hrb27C, Squid and Otu cooperatively regulate gurken RNA localization and mediate nurse cell chromosome dispersion in *Drosophila* oogenesis. *Development*, **131**, 1949–1958.
31. Geng, C. and Macdonald, P.M. (2006) Imp associates with Squid and Hrp48 and contributes to localized expression of gurken in the oocyte. *Mol. Cell Biol.*, **26**, 9508–9516.
32. Gagné, J.P., Hunter, J.M., Labrecque, B., Chabot, B. and Poirier, G.G. (2003) A proteomic approach to the identification of heterogeneous nuclear ribonucleoproteins as a new family of poly(ADP-ribose)-binding proteins. *Biochem. J.*, **371**, 331–340.
33. Matunis, M.J., Matunis, E.L. and Dreyfuss, G. (1992) Isolation of hnRNP complexes from *Drosophila melanogaster*. *J. Cell Biol.*, **116**, 245–255.
34. Burd, C.G. and Dreyfuss, G. (1994) RNA binding specificity of hnRNP A1: significance of hnRNP A1 high-affinity binding sites in pre-mRNA splicing. *EMBO J.*, **13**, 1197–1204.
35. Peritz, T., Zeng, F., Kannanayakal, T.J., Kilk, K., Eiríksdóttir, E., Langel, U. and Eberwine, J. (2006) Immunoprecipitation of mRNA-protein complexes. *Nature Protocol*, **1**, 577–580.
36. Morin, X., Daneman, R., Zavortink, M. and Chia, M. (2001) A protein trap strategy to detect GFP-tagged proteins expressed from their endogenous loci in *Drosophila*. *Proc. Natl Acad. Sci. USA*, **98**, 15050–15055.
37. Prasanth, K., Rajendra, T., Lai, A.K. and Lakhota, S.C. (2000) Omega speckles – a novel class of nuclear speckles containing hnRNPs associated with noncoding hsr-omega RNA in *Drosophila*. *J. Cell Sci.*, **113**, 3485–3497.
38. Expert-Bezançon, A., Sureau, A., Durosay, P., Salesse, R., Groeneveld, H., Lecaer, J.P. and Marie, J. (2004) HnRNP A1 and the SR proteins ASF/SF2 and SC35 have antagonistic functions in splicing of {beta}-tropomyosin exon 6B. *J. Biol. Chem.*, **279**, 38249–38259.
39. Garbe, J.C. and Pardue, M.L. (1986) Heat shock locus 93D of *Drosophila melanogaster*: a spliced RNA most strongly conserved in the intron sequence. *Proc. Natl Acad. Sci. USA*, **83**, 1812–1816.
40. Inoue, K., Hoshijima, K., Higuchi, I., Sakamoto, H. and Shimura, Y. (1992) Binding of the *Drosophila* transformer and transformer-2 proteins to the regulatory elements of doublesex primary transcript for sex-specific RNA processing. *Proc. Natl Acad. Sci. USA*, **89**, 8092–8096.
41. Shen, J., Beall, C.J. and Hirsh, J. (1993) Tissue-specific alternative splicing of the *Drosophila* dopa decarboxylase gene is affected by heat shock. *Mol. Cell Biol.*, **13**, 4549–4555.
42. Fahrer, J., Kranaster, R., Altmeyer, M., Marx, A. and Bürkle, A. (2007) Quantitative analysis of the binding affinity of poly(ADP-ribose) to specific binding proteins as a function of chain length. *Nucleic Acids Res.*, **35**, e143.
43. Zhu, J., Mayeda, A. and Krainer, A.R. (2001) Exon identity established through differential antagonism between exonic splicing silencer-bound hnRNP A1 and enhancer-bound SR proteins. *Mol. Cell*, **86**, 1351–1361.
44. Martinez-Contreras, R., Fiset, J.F., Nasim, F.U., Madden, R., Cordeau, M. and Chabot, B. (2006) Intronic binding sites for hnRNP A/B and hnRNP F/H proteins stimulate pre-mRNA splicing. *PLoS Biology*, **4**, 21.
45. Yost, H.J. and Lindquist, S. (1986) RNA splicing is interrupted by heat shock and is rescued by heat shock protein synthesis. *Cell*, **45**, 185–193.
46. Bond, U. (1988) Heat shock but not other stress inducers leads to the disruption of a subset of snRNPs and inhibition of *in vitro* splicing in HeLa cells. *EMBO J.*, **7**, 3509–3518.
47. Shin, C., Feng, Y. and Manley, J.L. (2004) Dephosphorylated SRp38 acts as a splicing repressor in response to heat shock. *Nature*, **427**, 553–558.
48. Malanga, M., Czuby, A., Girstun, A., Staron, K. and Althaus, F.R. (2008) Poly(ADP-ribose) binds to the splicing factor ASF/SF2 and regulates its phosphorylation by DNA topoisomerase I. *J. Biol. Chem.*, **283**, 19991–19998.
49. Kotova, E., Jarnik, M. and Tulin, A.V. (2009) Poly (ADP-Ribose) polymerase 1 is required for protein localization to Cajal body. *PLoS Genet.*, **5**, e1000387.